



## Original Research

## XPO1 inhibition with selinexor synergizes with proteasome inhibition in neuroblastoma by targeting nuclear export of IκB



Basia Galinski<sup>a,\*</sup>, Marcus Luxemburg<sup>a</sup>, Yosef Landesman<sup>b</sup>, Bruce Pawel<sup>c</sup>, Katherine J. Johnson<sup>d</sup>, Stephen R. Master<sup>d</sup>, Kevin W. Freeman<sup>e</sup>, David M. Loeb<sup>f</sup>, Jean M. Hébert<sup>g,a</sup>, Daniel A. Weiser<sup>a,f</sup>

<sup>a</sup> Department of Genetics, Albert Einstein College of Medicine, 1300 Morris Park Avenue Ullmann 813 Bronx, NY 10461, United States

<sup>b</sup> Karyopharm Therapeutics, Newton MA, United States

<sup>c</sup> Clinical Pathology, Children's Hospital Los Angeles, United States

<sup>d</sup> Pathology and Laboratory Medicine, University of Pennsylvania, United States

<sup>e</sup> Genetics, Genomics and Informatics, University of Tennessee Health Science Center, United States

<sup>f</sup> Department of Pediatrics, Albert Einstein College of Medicine, United States

<sup>g</sup> Department of Neuroscience, Albert Einstein College of Medicine, United States

## ARTICLE INFO

## Keywords:

Neuroblastoma  
Exportin-1  
Selinexor  
Bortezomib  
IκB  
NF-κB

## ABSTRACT

Across many cancer types in adults, upregulation of the nuclear-to-cytoplasmic transport protein Exportin-1 (XPO1) correlates with poor outcome and responsiveness to selinexor, an FDA-approved XPO1 inhibitor. Similar data are emerging in childhood cancers, for which selinexor is being evaluated in early phase clinical studies. Using proteomic profiling of primary tumor material from patients with high-risk neuroblastoma, as well as gene expression profiling from independent cohorts, we have demonstrated that XPO1 overexpression correlates with poor patient prognosis. Neuroblastoma cell lines are also sensitive to selinexor in the low nanomolar range. Based on these findings and knowledge that bortezomib, a proteasome inhibitor, blocks degradation of XPO1 cargo proteins, we hypothesized that combination treatment with selinexor and bortezomib would synergistically inhibit neuroblastoma cellular proliferation. We observed that selinexor promoted nuclear retention of IκB and that bortezomib augmented the ability of selinexor to induce cell-cycle arrest and cell death by apoptosis. This synergy was abrogated through siRNA knockdown of IκB. The synergistic effect of combining selinexor and bortezomib in vitro provides rationale for further investigation of this combination treatment for patients with high-risk neuroblastoma.

## Introduction

Neuroblastoma is the most common extracranial solid tumor of childhood [1]. For those with high-risk neuroblastoma, defined by clinicobiological features, including stage, patient age at presentation, and *MYCN* copy number status, survival has remained poor. A subset of patients with high-risk disease succumbs to cancer progression within 18 months of diagnosis [2,3], yet there are currently no validated features to identify these ultra-high risk patients at diagnosis. Greater understanding of the unique tumor biology of patients who have the poorest outcomes has the potential to provide insight about novel treatment approaches [4].

Across a range of malignancies, high expression of Exportin-1 (XPO1) correlates with inferior outcome [5–10]. XPO1 is a nuclear transport

protein that shuttles over 200 cell regulatory proteins from the nucleus to the cytoplasm [11,12]; there is no other exportin that provides the same function [13,14]. The location and availability of proteins in the nuclear or cytoplasmic compartments affects normal cell homeostasis, signaling pathways, and protein degradation. Selinexor, a selective inhibitor of nuclear export (SINE) agent, blocks XPO1 function and induces nuclear localization of tumor suppressor and growth regulatory proteins, as well as oncoprotein encoding mRNAs. In addition, selinexor inhibits the expression of DNA damage repair proteins. Its efficacy in patients with diffuse large B-cell lymphoma and multiple myeloma has led to FDA approval [15–19], and its activity has been preliminarily assessed in neuroblastoma [10].

One XPO1 cargo protein, IκB is an inhibitor of NF-κB, a transcription factor that activates pro-survival signaling pathways in cancer, in-

**Abbreviations:** XPO1, Exportin-1; SEL, selinexor; VEH, vehicle; Nuc, nuclear compartment; Cyto, cytoplasmic compartment; BTZ, bortezomib; CI, combination index; Fa, fraction affected; NT, non-targeting siRNA pool; CO, Combination treatment; R.LU.s, relative luciferase units.

\* Corresponding author.

E-mail address: [basia.galinski@einsteinmed.org](mailto:basia.galinski@einsteinmed.org) (B. Galinski).

<https://doi.org/10.1016/j.tranon.2021.101114>

Received 8 February 2021; Received in revised form 12 April 2021; Accepted 23 April 2021

1936-5233/© 2021 The Authors. Published by Elsevier Inc. This is an open access article under the CC BY-NC-ND license

(<http://creativecommons.org/licenses/by-nc-nd/4.0/>)

cluding neuroblastoma [20–23]. Cytoplasmic I $\kappa$ B is phosphorylated and tagged for degradation by the proteasome, promoting NF- $\kappa$ B nuclear translocation and eliminating an important negative regulator of NF- $\kappa$ B activity. Selinexor is known to block I $\kappa$ B export, and further targeting of NF- $\kappa$ B activity has been achieved with bortezomib, a proteasome inhibitor which has also been previously investigated in neuroblastoma [22–26].

In this study, we tested the hypothesis that selinexor and bortezomib act synergistically to both stabilize I $\kappa$ B and to promote its nuclear localization, leading to decreased NF- $\kappa$ B activity and neuroblastoma cell death. First, we found that XPO1 is highly abundant in patients with neuroblastoma who have the poorest outcomes. Next, we demonstrated that XPO1 inhibition, in combination with proteasome inhibition, synergistically impaired neuroblastoma growth in vitro and promoted apoptosis. This synergy was dependent on I $\kappa$ B-mediated inhibition of NF- $\kappa$ B activity. Our work suggests a potential new combination strategy for the treatment of patients with highly aggressive neuroblastoma.

## Materials and methods

### Tumor profiling

We performed ion intensity-based label-free semiquantitative proteomic profiling on de-identified primary tumor material from 50 patients with uniformly treated high-risk neuroblastoma (defined as greater than 18 months of age and International Neuroblastoma Staging System stage 4 (presence of distant metastases), half of whom were long term survivors (>3 years) and half of whom died <18 months from diagnosis of disease progression. Samples were obtained from the Children's Oncology Group clinically annotated Biospecimen Bank and institutional review board exempt status was granted. A board-certified pediatric pathologist with expertise in neuroblastoma confirmed histologic diagnoses and highlighted the best preserved and most representative regions of tumor sections (e.g., nodules in ganglioneuroblastoma) for subsequent analyses.

Using 5- to 10-mm-thick formalin-fixed paraffin-embedded tumor sections on a glass slide, antigen retrieval methods were used to extract one microgram of protein from the tissue [27]. Proteins were digested with trypsin using Filter Aided Sample Preparation as previously described and peptides were desalted using StageTips prior to LC-MS/MS analysis [28,29]. Proteolytic peptides were separated on a 60 cm  $\times$  75  $\mu$ m column packed in house with 4  $\mu$ m C12 Jupiter Proteo beads (Phenomenex, CA, USA) that were maintained at 50°C. Peptides were separated at a flow rate of 300 nL/min with a 90-min gradient of 2% to 42% acetonitrile with 0.5% acetic acid. Eluted peptides were detected with an LTQ Orbitrap Hybrid Mass Spectrometer (Thermo Scientific, MA, USA) with a full mass range of  $m/z = 370$ –2000. The 5 most intense precursor masses were selected for fragmentation in the linear ion trap.

Proteomics data were searched against the human UniProt database with MaxQuant v1.3.0.5 using a 1% false discovery rate. Identified proteins with nonsignificant mapping ( $p$ -value>0.05) and high missing rate across samples (missing data $\geq$ 0.2) were excluded from analysis. Data were then normalized using central tendency measure and missing data were imputed using singular value decomposition using R functions from InfernoRDN software (v1.1.5438, <http://omics.pnl.gov/software/infernordn>) [30,31]. Two samples were excluded due to high data missing rate and low correlation with other samples. Remaining samples were clustered using the pvclust (v1.3–2) R package [32]. We used hierarchical clustering with an average agglomeration method and correlation distance measure. To determine stability and significance of the clustering results, we performed bootstrap resampling of the data with 1000 replications.

To perform Kaplan–Meier analyses, we utilized the R2: Genomics Analysis and Visualization Platform (<http://r2.amc.nl>). Individual

databases used to investigate correlations and survival analyses are found within the R2: Genomics Analysis and Visualization Platform, with appropriate citations in the text and notation of individual databases in the figure legend.

A paraffin embedded tissue microarray was constructed which consisted of duplicate punches of 185 neuroblastic tumors archived at The Children's Hospital of Philadelphia from 1987 to 2003. Staining information was obtained for 149 samples, which consisted primarily of poorly differentiated neuroblastomas. Control tissues included brain, adrenal, placenta and tonsil. Immunohistochemical staining was performed using mouse anti-human [CRM1 Santa Cruz] according to manufacturer's protocol. Each sample was scored by the same pathologist and was designated as "0" when no staining was present, "1" when 0–10% of cells stained positively, "2" when 10–90% of tumors stained positively and "3" when greater than 90% of cells stained positively. Only cells of neuroblastic lineage were evaluated for XPO1 staining. These cells included immature neuroblasts, maturing neuroblasts, and mature ganglion cells. Stromal cells, including fibroblasts, Schwann cells, endothelial cells and pericytes were not counted, nor were infiltrating inflammatory cells.

### Cell culture and reagents

STR authenticated cell lines IMR5, NLF, SKNSH, EBC1, LAN5, NB16, NB1643, CHLA15, CHLA20, and hTERT-immortalized RPE1 were obtained through the Children's Oncology Group Cell Culture and Xenograft Repository (<https://www.cccells.org/>, powered by Alex's Lemonade Stand) and the Children's Hospital of Philadelphia. Cell lines were maintained in RPMI-1640 or IMDM media (Gibco) with 10% FBS and 1% penicillin/streptomycin in 5% CO<sub>2</sub> atmosphere at 37 °C. Selinexor was obtained from Karyopharm Therapeutics through a material transfer agreement. Bortezomib (LC laboratories) was purchased and both agents were resuspended into DMSO and aliquoted into stocks stored at –20 °C. DMSO was used as vehicle control for all experiments. Knockdown of I $\kappa$ B through siRNA set of 4 targeting oligonucleotides (Q-004765-00-0010) were purchased along with a control non-targeting pool (D-001810-10-05 Horizon), use 2 of the 4 single targeting siRNA oligonucleotides used in experiments were based on I $\kappa$ B knockdown efficiency. NF- $\kappa$ B response element luciferase plasmid and GFP control plasmid (Lonza pMAXGFP D-00076 a gift from the Sharp lab) were used with Nano-Glo Dual-Luciferase Kit (Promega N1111). Plasmid and siRNA transfections used Lipofectamine 3000 and Lipofectamine 2000 respectively (Thermo Scientific). siRNAs were transfected for 24 h prior to drug treatment. Plasmids were transfected for 48 h prior to drug treatment for 2 h followed by 4 h stimulation with TNF $\alpha$  (R&D Systems 210-TA) at 20 mg/ $\mu$ L. All plating utilized a control lane with transfection reagent added for baseline absorbance values. Luciferase assays were read after 6 h of drug treatment in total, on a plate reader (Biotek Cytation 5) for each plasmid. All experiments and assays were performed in triplicate with three technical replicates.

### MTT assay and evaluation of drug interaction

Cell proliferation was measured using Cell Titer 96 AQueous One Solution (Promega) in a 96-plate format. Assays were read 48 h post treatment with drug or siRNAs on a Wallac plate reader at an absorbance of 490 nm. Ten doses of single agent selinexor and bortezomib were tested to determine IC<sub>50</sub> concentrations and were calculated using exponential regression in GraphPad Prism software. For assessment of synergy, 8 concentrations of drug, starting at 6.25 nM with sequential doubling to 800 nM, were used in a 1:1 ratio. This provided combination dose response curves ranging from 100% cell viability to 0% cell viability. Determination of relative viability was calculated as seen previously [33]. Isobologram analysis and Combination Index were calculated through

CompuSyn software. Data show a representation of 3 independent experiments.

#### Western blot analysis

Neuroblastoma cells were scraped and whole cell protein was extracted using RIPA buffer (100 mM NaCl, 10 mM Tris at pH 7.5, 0.1% SDS, 0.5% Deoxycholate, 1% NP40) and protease inhibitor cocktail (cComplete Tablets EASY Pack Protease Inhibitor Cocktail Tablets, Roche). For fractionation of cell lysates we utilized homemade lysis buffers (Lysis buffer 1–50 mM Tris-HCl, 150 mM NaCl, 20 mM NaF, 1 mM EDTA, 1 mM EGTA, 0.5% NP-40, 10% Glycerol while Lysis buffer 2 contained the above but 500 mM NaCl and 1% NP-40) with increasing salt and detergent concentrations as well as increasing centrifugation with protease inhibitor cocktail and phosphatase inhibitor (Phosphatase Inhibitor Cocktail 2 P5726 Sigma). Nuclear pellets were sonicated 3 times at 15% power for 5 s to rupture the nucleus. Protein quantification was performed by Bradford Assay (Bio-Rad) and 50ug of protein was run on a 12% SDS-PAGE gel (GeneScript Express Plus PAGE Gel) and transferred to Polyvinylidene fluoride (PVDF) membrane for 1 hr at 4 °C. Licor TBS blocking buffer (927-50000) was used with washes of TBS + Tween-20 (0.1%) and primary antibodies incubated at 1:500–1:1000 and secondary antibodies at 1:8000 for 1 h time. Imaging of blots was performed on Licor Odyssey Imaging machine with quantifications of band intensity performed on Image Studio Lite software.

#### Antibodies

Primary antibodies used for Western blotting as well as immunofluorescence are as follows: XPO1 (46249S), GAPDH (14C10), NF- $\kappa$ B(3035S), PARP/C-PARP (9542S), p-NF- $\kappa$ B, Tubulin (2148S), Vinculin (E1E9V), and Histone H2AX (D17A3) were purchased from Cell Signaling, I $\kappa$ B $\alpha$  (ab7217) was purchased from Abcam. Li-COR IRDye secondary antibodies 680 and 800 donkey anti-mouse and donkey anti-rabbit were used for detection of protein bands on Odyssey Li-COR machine. For immunofluorescence, Alexa fluorescent secondary antibody goat anti-rabbit 488 was used.

#### Flow cytometry

Cells were grown on 10 cm plates and exposed to drugs in single and combination for 48 h. Doses of selinexor and bortezomib, derived from the dose response curves, were 40 nM (IMR5, NLF) or 60 nM (SKNSH) and 4 nM (all cell lines), respectively. All experiments were read on the BD LSRII UP in the institution's core facilities each sample was read for 10,000 events. For apoptosis, cells were extract at 48 h and labeled following the instructions on the Annexin-V PI kit (Thermo Fisher). Non-treated cells were combined with heatshocked non-treated cells at 60 °C for 1 min followed by 37 °C for 1 h to be used for a gating control on the flow cytometer. FlowJo software version 9 was used for analysis of populations that were viable, dead, or in an early or late phase of apoptosis. For cell cycle experiments, cells were labeled with BrdU at 48hours and incubated for 2 h at 37 C. They were then collected and labeled with the BD Pharmingen BrdU FITC kit. Flow Jo software version 9 was used to indicate what phase cells were in.

#### Immunofluorescence

Cells were grown on coated bovine collagen (Gibco A1064401) coverslips overnight and exposed to selinexor or vehicle for 1  $\mu$ M for 6 h. Following treatment cells were fixed with 4% paraformaldehyde and permeabilized with Saponin 0.2%. Fixed slides were blocked in 10% fetal bovine serum (FBS) and probed with primary and secondary antibodies. Prolong Antifade mounting medium with DAPI (Thermo Fisher) was used for mounting. Images were taken with Leica SP8 con-

focal and Volocity software (PerkinElmer) was used to quantify nuclear and cytoplasmic staining intensity. For each experiment greater than 100 nuclei were used for quantitative measures from 3 independent experiments.

#### Statistics

For all experiments of 3 independent experiments or greater, statistical significance was determined by using Prism Software for a student's *t*-test between 2 groups and between multiple groups, one-way ANOVA followed by Tukey's for multiple comparisons. A *P*-value of less than 0.05 was considered to be significant.

#### Results

##### *XPO1 is highly expressed in patients who have the poorest outcomes*

Primary tumor samples from patients with high-risk neuroblastoma were used to perform top-down proteomics to compare profiles of patients who were long-term survivors (controls: >3-year survival) with patients who died rapidly of disease progression (cases <18-month survival). These data demonstrate that XPO1 is one of the most highly abundant proteins in patients who have the most aggressive disease (Fig. 1a and b, Supplemental Table 1). XPO1 was of interest to our group because of the increased recognition of its key role in cellular homeostasis, the correlation of high protein expression with inferior outcome in multiple cancer types, and the availability of a pharmacologic agent to target it [5,34–36]. We then utilized an independent publicly available dataset from R2: Neuroblastoma Genomics Analysis and Visualization Platform (<https://hgserver1.amc.nl/cgi-bin/r2/main.cgi>) to create a Kaplan-Meier survival curve of the Kocak data set, comparing survival between patients with neuroblastoma whose tumors had low versus high levels of XPO1. Unlike the proteomics data set that analyzed tumors from patients with high-risk neuroblastoma, the Kocak data set includes patients with neuroblastoma across all risk groups, excluding patients with stage 4S disease. The event-free survival probability of patients with high XPO1 expression was inferior to those with low XPO1 expression (raw *p*-value of 2.5e-05 and Bonferroni correction of 9.9e-03) (Fig. 1c), demonstrating that high XPO1 expression consistently correlates with inferior survival. We next surveyed an independent neuroblastoma tumor microarray to assess XPO1 immunohistochemical staining and verify transcriptomic data. Eighty-nine percent of samples stained positive, with a range of intensity from 1+ to 3+ (Fig. 1d). Tumor cores scored as 0+ (no staining) were primarily ganglioneuromas or poor quality specimens. These data demonstrate that high XPO1 protein expression and high gene expression, regardless of neuroblastoma risk grouping, correlate with inferior outcome, and that XPO1 is nearly universally present in tumor tissue.

##### *Selinexor reduces cell viability in a heterogeneous panel of neuroblastoma cell lines with a range of XPO1 expression*

A panel of nine neuroblastoma cell lines with molecular diversity were analyzed for XPO1 expression by immunoblotting. With the exception of SKNSH, XPO1 expression was substantially greater in neuroblastoma cell lines than in immortalized, nontransformed retinal pigmented epithelial (RPE1) cells (Fig. 2a). We then generated selinexor dose response curves. The IC<sub>50</sub> range for the neuroblastoma cell lines ranged from 4 to 312 nM, whereas RPE1 was relatively insensitive, with an IC<sub>50</sub> of 41  $\mu$ M (Fig. 2b, Supplemental Fig. 1). Sensitivity to selinexor was independent of cell line biologic features that are relevant in human disease, including MYCN copy number status (IMR5, LAN5, NLF and NB1643 are MYCN amplified). Recognizing that nuclear export of I $\kappa$ B is mediated by XPO1, we analyzed changes in nuclear and cytoplasmic localization of I $\kappa$ B with selinexor. Using immunofluorescence and confocal microscopy, we found that selinexor treatment results in

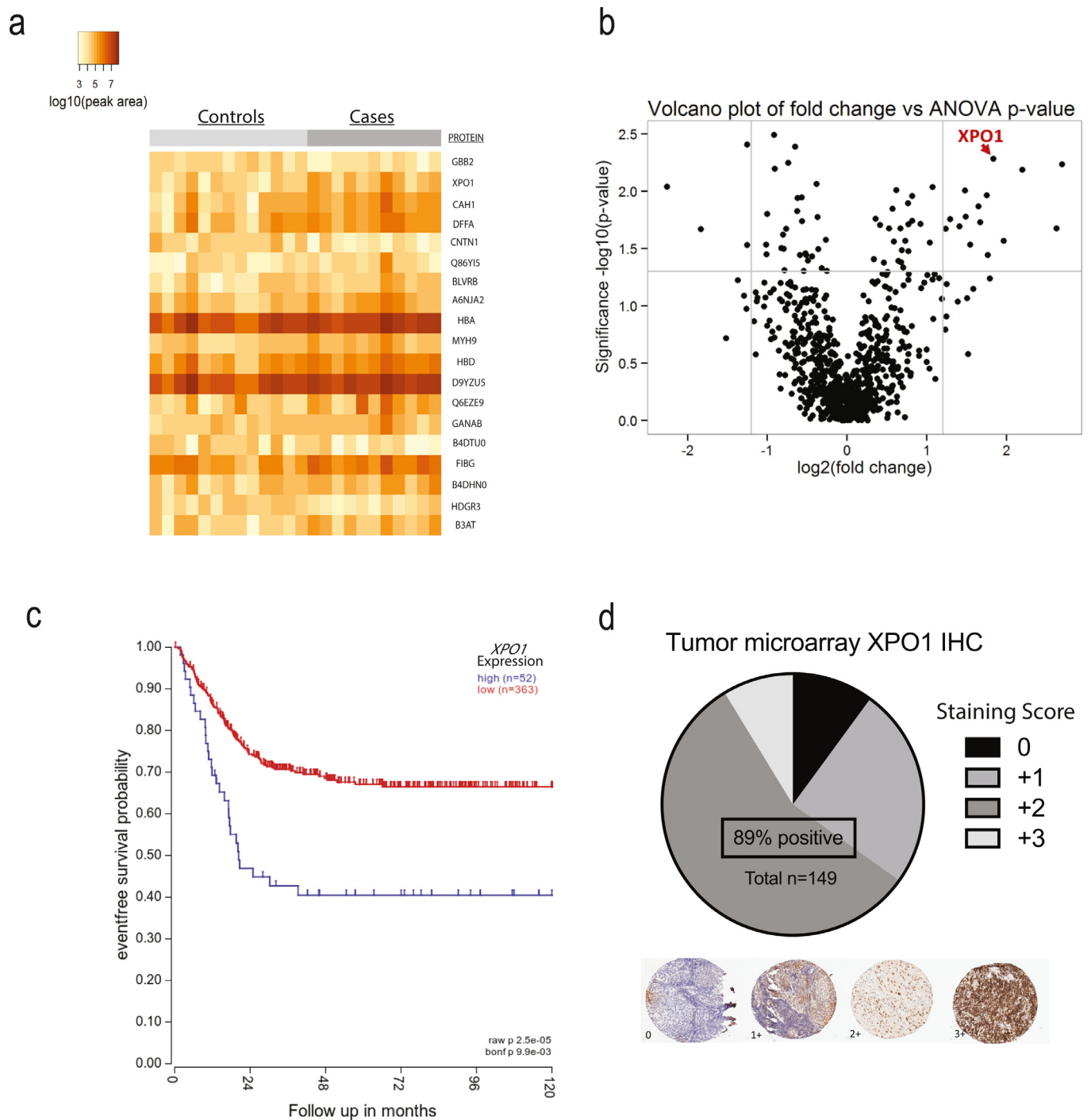


**Fig. 1.** High XPO1 expression correlates with poor patient outcome in neuroblastoma. **a.** Clustering based on outcome for patients with high-risk neuroblastoma, demonstrating differential abundance of proteins, including XPO1 as a top candidate. **b.** Volcano plot showing differentially abundant proteins in patients with neuroblastoma who survived (negative X-axis plot points) compared to patients who succumbed to disease (positive X-axis plot points) and highlighting XPO1 as significantly (Y-axis) increased in patients who ultimately succumb to disease. Gray solid line indicates 1% FDR. **c.** Long-term event-free survival of patients with neuroblastoma stratified by XPO1 expression using R2: Genomics Analysis and Visualization Platform (<http://r2.amc.nl>), Kocak cohort (N >250). **d.** Pie chart demonstrating the breakdown of XPO1 immunohistochemical (IHC) staining intensity in a tumor microarray of neuroblastoma samples from patients across all risk groups. 89% of 149 tumors stained positive, with the range of intensity from 0 (none) to 3+ (strong). The array was originally scanned at 200x magnification.

a statistically significant increase of IκB in the nucleus (*p*-value <0.05, Fig. 2c and d), while no change in IκB abundance was appreciated in the cytoplasm. The increased nuclear retention of IκB caused by selinexor was confirmed by immunoblotting of nuclear and cytoplasmic proteins (Fig. 2e). We did not identify a correlation between IκB abundance or localization and sensitivity to selinexor.

*The combination of selinexor and bortezomib is synergistic in neuroblastoma cell lines*

Selinexor has a fairly favorable toxicity profile when used clinically in adult patients [37], though children may be more prone to dose-limiting toxicities. We therefore considered combinatorial treat-

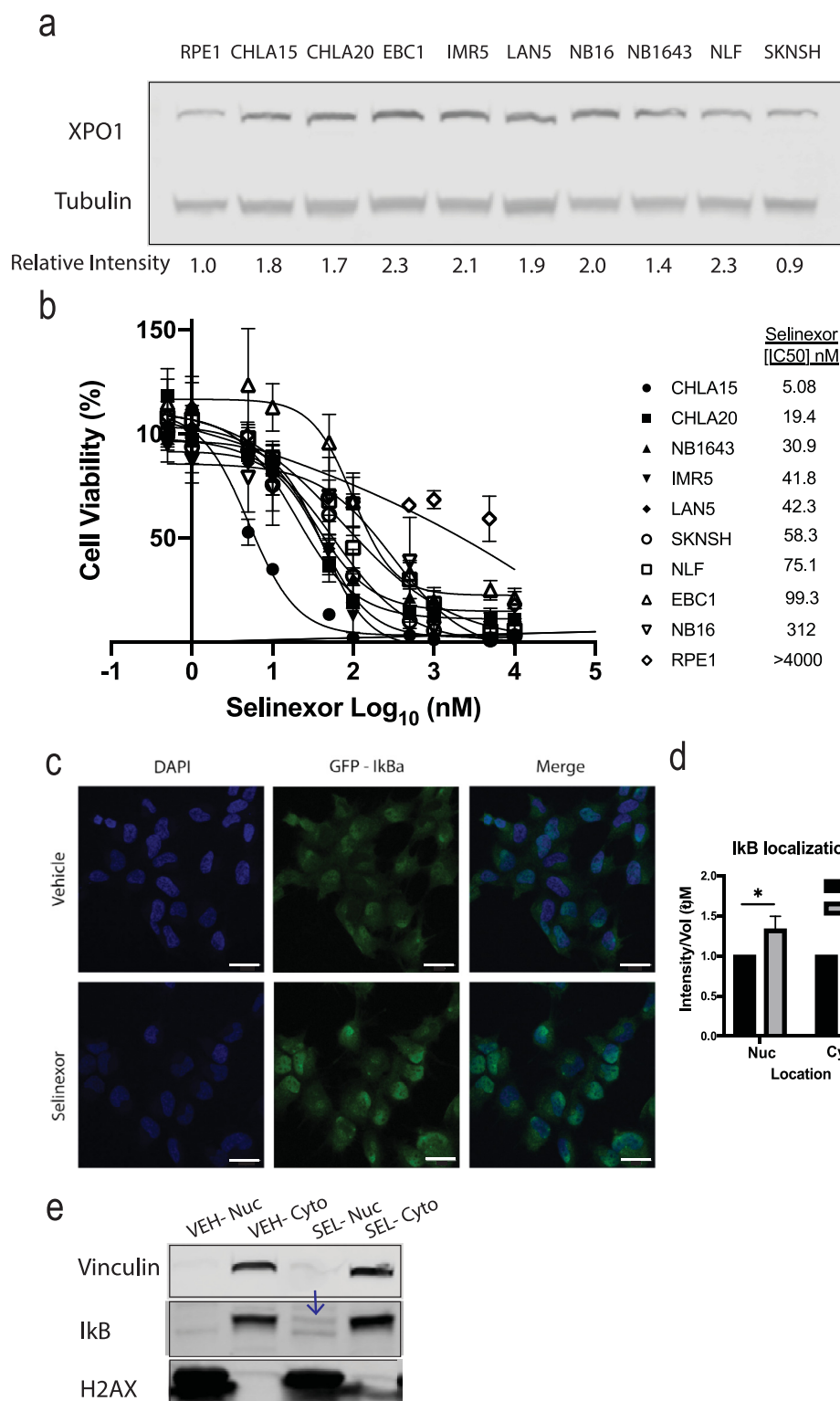


**Fig. 2.** Pharmacologic inhibition of XPO1 with selinexor suppresses neuroblastoma growth in vitro. **a.** Western blot showing a panel of neuroblastoma cell lines with generally high relative XPO1 expression compared to RPE1. Tubulin was used as loading control for each cell lysate. **b.** Selinexor dose response curves demonstrate nanomolar range sensitivity across all neuroblastoma cell lines and independent of protein expression. RPE1 is relatively insensitive to selinexor with an IC<sub>50</sub> of 41 μM. **c.** Immunofluorescence of a representative cell line using confocal microscopy shows increased IκB (green GFP-labeled) in the nucleus in response to selinexor. Nuclear staining is shown in blue by DAPI. **d.** Quantification using Volocity demonstrates the abundance of IκB (GFP signal) in the nuclear (Nuc) compartment was significantly higher with selinexor (SEL) compared to vehicle (VEH) (*p*-value: < 0.05). No change was observed in the cytoplasmic (Cyto) abundance of IκB in response to selinexor. **e.** Western blot showing increased IκB in the nuclear compartment (indicated with an arrow) with fractionation using Vinculin as a cytoplasmic marker and Histone H2AX as a nuclear marker. Data shown are representative of 3 experiments with 6 technical replicates (dose response curves) or 3 experimental and technical replicates (IF/Western blots). Densitometry values are representative of 3 independent experiments.

ment strategies to augment selinexor activity without the need for dose escalation. Bortezomib, a proteasome inhibitor, has been evaluated in neuroblastoma with single agent in vitro IC<sub>50</sub>s also in the nanomolar range [25], though results from clinical studies have shown less promising results [38]. Since bortezomib inhibits NF-κB signaling in a distinct manner from selinexor, we hypothesized that the combination of selinexor and bortezomib would more effectively diminish NF-κB-related

pro-survival signaling in neuroblastoma. IMR5, NLF and SKNSH neuroblastoma cell lines were selected for their diversity of molecular features, including *MYCN* amplification (IMR5 and NLF), wild type *TP53* (IMR5 and SKNSH), and differential abundance of XPO1 (Fig. 2a). To assay for synergy between bortezomib and selinexor, we used combination index (CI) and isobologram analyses. CI values less than 1 indicate synergy, which is present across multiple dose ranges and cell lines (Fig. 3a-c)

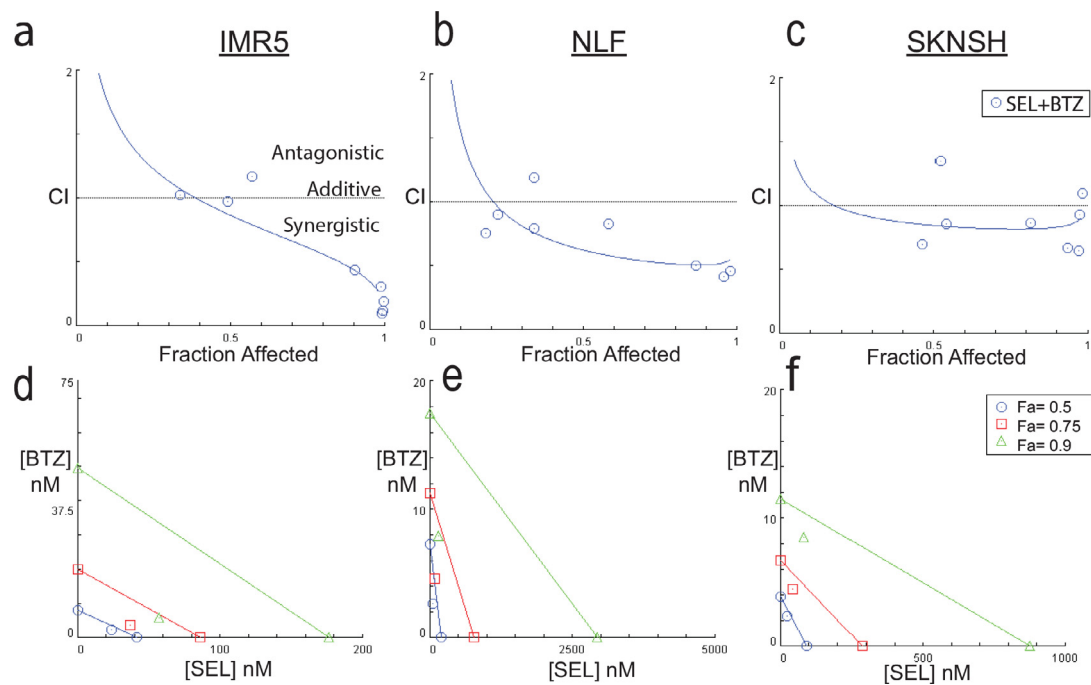


**Fig. 3.** Analysis of selinexor and bortezomib in neuroblastoma cells demonstrates synergy. a–c. Combination index (CI) is presented as a function of the fraction affected (Fa) for equipotent fixed-ratio combinations of selinexor and bortezomib (SEL+BTZ). Points below a CI of 1, the line of additivity, are considered synergistic, whereas a CI  $\geq 1.1$  is considered antagonistic. d–f. An alternative representation of synergy through isobolograms. The 3 diagonal lines of additivity represent the Fa at 0.5 (blue), 0.75 (red), and 0.9 (green) at corresponding treatment doses. Synergy is represented by the colored point for each line of additivity (blue circle, red square, green triangle) falling below the line of additivity, as demonstrated across cell lines. Data shown are representative of 3 experiments with 6 technical replicates.

and suggests that lower doses of both drugs, compared to single agent concentrations, can achieve high anti-tumor activity and potentially reduce toxicity. We then applied isobologram analyses at effect levels of 0.5, 0.75, and 0.9 growth inhibition (Fig. 3d–f). The isobole of the combination was below the line of additivity at all effect levels and across all cell lines, confirming the synergy of bortezomib and selinexor regardless of underlying cell line biology.

#### Selinexor and bortezomib promote cell cycle arrest and apoptosis

We next investigated the effects of selinexor and bortezomib on cell cycle arrest and apoptosis. Using BrdU labeling we found that selinexor monotherapy contributed to an increase in G1-0 arrest ( $p$ -value  $< 0.05$ ) and a corresponding decrease in cells in S phase ( $p$ -value  $< 0.05$ ). Combination treatment with selinexor and bortezomib enhanced G1-0 arrest in all cell lines, though this was statistically significant only in the *MYCN* non-amplified cell line, SKNSH ( $p$ -value  $< 0.05$ ) (Fig. 4a). We then proceeded to assess for apoptosis using Annexin-V labeling. Comparing the viable population between treatment conditions, we saw a significant decrease from single drug to combination ( $p$ -value  $< 0.001$  for selinexor or bortezomib vs. combination in IMR5;  $p$ -value  $< 0.01$  for selinexor vs. combination and  $p$ -value  $< 0.05$  for bortezomib vs. combination in NLF). We saw a statistically significant increase in total apoptotic cells with combination treatment compared with selinexor ( $p$ -value  $< 0.001$  in IMR5 and NLF,  $p$ -value  $< 0.05$  in SKNSH) and also compared with bortezomib ( $p$ -value  $< 0.001$  in IMR5,  $p$ -value  $< 0.05$  in NLF) (Fig. 4b). To support these findings, we utilized Western blotting to assess protein levels of the cleaved form of PARP (c-PARP), an early marker in the signal cascade for apoptosis. c-PARP was greatest in cells treated with the combination of selinexor and bortezomib, suggesting that they work cooperatively to induce apoptosis (Fig. 4c).

#### Mechanistic assessment of selinexor-bortezomib combination therapy demonstrates the crucial role of I $\kappa$ B in diminishing Nf- $\kappa$ B activity and cellular proliferation

Finally, we directly tested our hypothesis that I $\kappa$ B is critical to the synergy seen between selinexor and bortezomib. Nuclear retention of I $\kappa$ B is a key step in the inhibitory regulation of NF- $\kappa$ B signaling pathway and one that is most pronounced with combination treatment [39,40]. Using an NF- $\kappa$ B luciferase assay in two cell lines that were amenable to transfection, we first demonstrated that selinexor and bortezomib as single agents led to decreased NF- $\kappa$ B signaling compared to vehicle when stimulated with TNF $\alpha$ , a known activator of NF- $\kappa$ B activity [41]. We then showed that combination treatment resulted in the lowest amount of NF- $\kappa$ B activity (Fig. 5a). Next, we sought to determine if I $\kappa$ B was necessary for this effect. We found that siRNA knockdown of I $\kappa$ B, using 2 distinct siRNA constructs, eliminated the treatment effect in IMR5 and NLF cell lines, while a nontargeting siRNA had no effect. Specifically, selinexor treatment with siRNA knockdown was similar to vehicle without I $\kappa$ B knockdown (IMR5 – SEL non-targeting vs siRNA1:  $p$ -value  $< 0.01$ , non-targeting vs siRNA2  $p$ -value  $< 0.05$ ; NLF – SEL non-targeting vs siRNA1:  $p$ -value  $< 0.05$ , non-targeting vs siRNA2  $< 0.01$ ), bortezomib and combination treatment with siRNA knockdown of I $\kappa$ B demonstrated relative increased proliferation activity (IMR5- BTZ/CO non-targeting vs siRNA1:  $p$ -value  $< 0.01$ , non-targeting vs siRNA2  $< 0.05$ ; NLF- BTZ non-targeting vs siRNA1:  $p$ -value  $< 0.001$ , CO non-targeting vs siRNA1:  $p$ -value  $< 0.05$ , non-targeting vs siRNA2:  $p$ -value  $< 0.05$ ) (Fig. 5b and c). These results reflect the key regulatory role of I $\kappa$ B in the NF- $\kappa$ B signaling pathway and suggest one mechanistic explanation of the synergy between selinexor and bortezomib.

#### Discussion

Patients with the most highly aggressive neuroblastoma, often referred to as those with ultra-high-risk neuroblastoma, have dismal out-

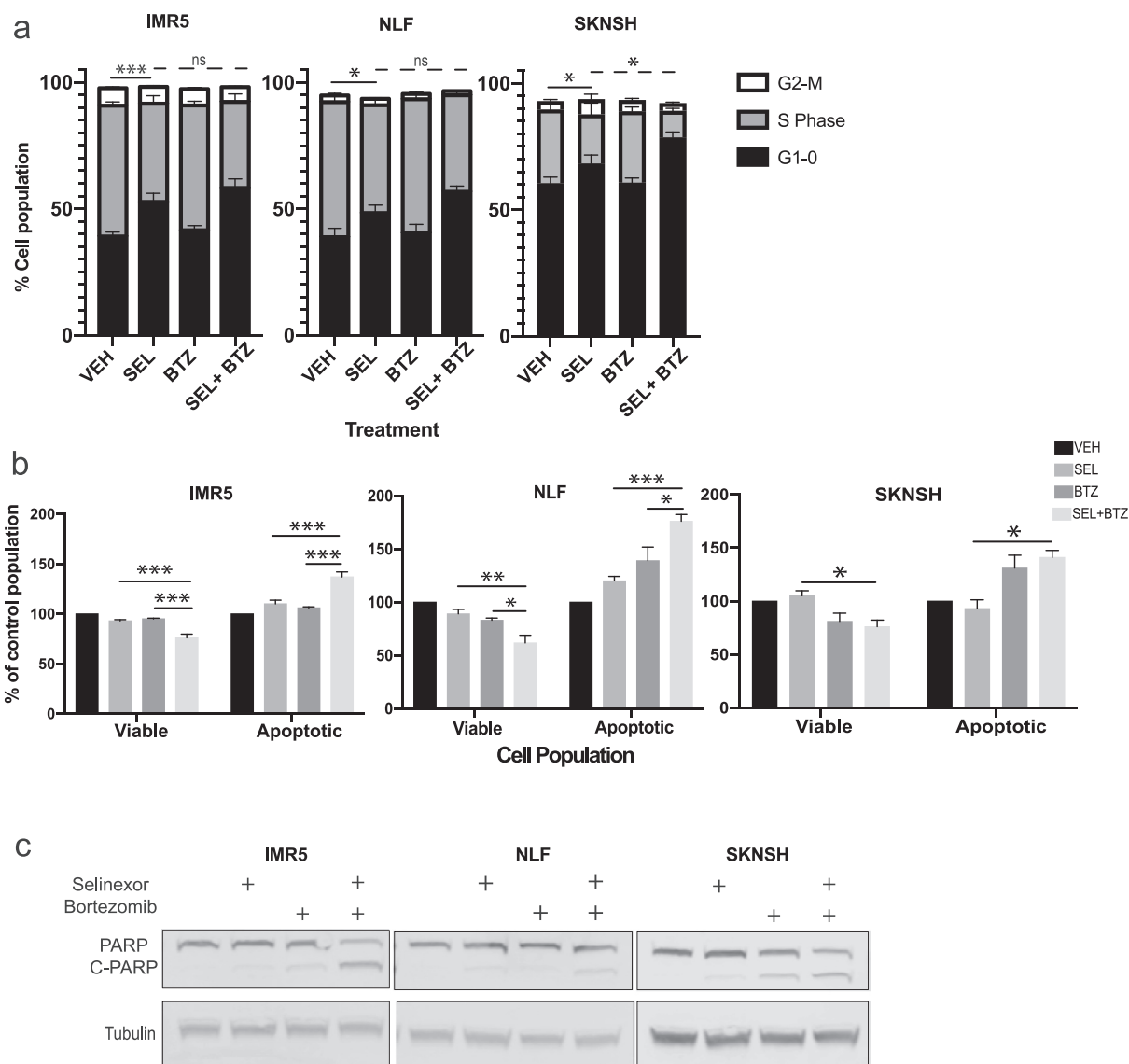


**Fig. 4.** Bortezomib augments selinexor-induced cell cycle arrest and combination therapy promotes apoptosis. Neuroblastoma cell lines IMR5, NLF, and SKNSH were treated with vehicle, selinexor, bortezomib, or combination for 48 h and stained for flow cytometry to evaluate cell cycle arrest and apoptosis. **a.** Cell cycle arrest using BrdU labeling shows that single agent selinexor increases G1-0 arrest ( $p$ -value <0.001 in IMR5,  $p$ -value <0.05 in NLF and SKNSH) and decreases S phase ( $p$ -value <0.001 in IMR5,  $p$ -value <0.05 in NLF, not significant (ns) in SKNSH), while bortezomib is not significantly different from vehicle. **b.** Annexin-V labeling of apoptosis demonstrates decreased cell viability with combination therapy in comparison to single agent, and there is a corresponding increase in apoptotic cell populations. **c.** Western blots showing that total c-PARP, an early signaling event of apoptosis, is most abundant in combination experiments compared to either single agent. Tubulin was used as a loading control for equal cell lysates. G1-0 comparison bars represent  $p$ -values corresponding to <0.05-\*, <0.01-\*\*, <0.001-\*\*\* between selinexor and vehicle in the 3 cell lines, while S phase comparison bars dashed lines: are ns (not significant) in IMR5 and NLF for selinexor compared to combination and in SKNSH <0.05-\*. These data are from 3 independent experiments with 3 technical replicates per condition.

comes. Up to 15% of patients with newly diagnosed high-risk neuroblastoma will die from disease progression within 18 months from diagnosis, and there is a clear imperative to better understand drivers of disease and develop novel approaches to management. We have demonstrated that XPO1 expression correlates with highly aggressive neuroblastoma and that patients with this form of the disease may benefit from a novel combinatorial treatment approach with selinexor and bortezomib. The synergistic effect of these agents addresses concerns about dose-limiting toxicities of selinexor [42], and accordingly, similar combination strategies have recently led to FDA approval of selinexor in multiple myeloma which may support its use in the pediatric patient population.

XPO1 is nearly universally expressed in neuroblastoma, including in the panel of cell lines used in our studies, though we did not identify

a correlation between expression level and sensitivity to selinexor. In addition, in one representative cell line pair, CHLA15 and CHLA20 derived from the same patient before and after treatment, respectively, the selinexor IC<sub>50</sub> values were comparable. These results suggests that drug sensitivity in patients would be independent of XPO1 expression even though expression can serve as a prognostic biomarker. Retrospective studies of XPO1 expression show how critical XPO1 is to the oncogenic process but with the lack of knowledge on how overexpression occurs, it is the cargo proteins and pathways thereof that remain the most promising for a therapeutic marker of response [43,44].

In neuroblastoma and other cancers, high transcriptional activity of NF-κB can be inhibited through IκB nuclear localization and stabilization [45–47]. Proteasome inhibitors, such as bortezomib, achieve this through preventing degradation of IκB, thereby maintaining IκB func-

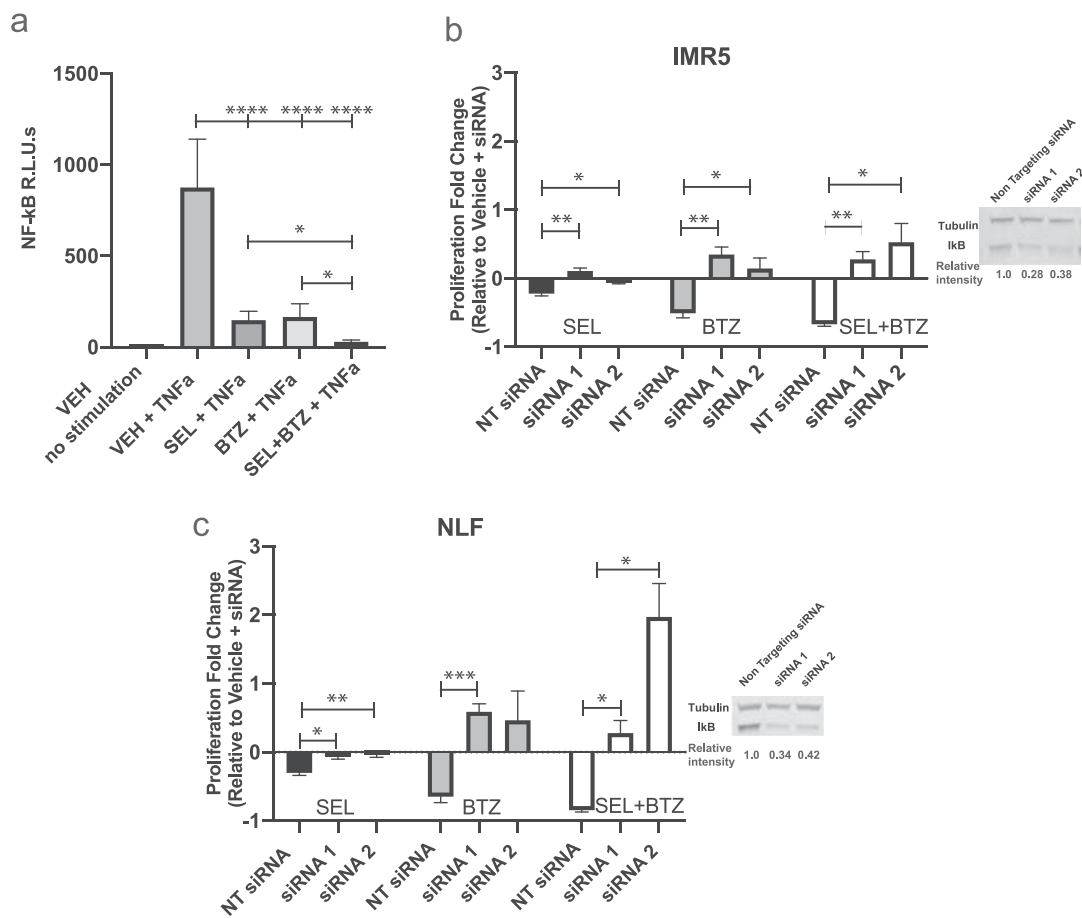


**Fig. 5.** Combination treatment with selinexor and bortezomib reduces NF-kB transcriptional activity, a process mediated through Ikb. **a.** NF-kB activity was measured as Relative Luciferase Units (R.L.U.s) in NLF neuroblastoma cell line using a luciferase reporter plasmid and GFP for transfection control. Each drug treatment condition received TNFa stimulation to provide a robust NF-kB signal. With selinexor, bortezomib, and combination treatment, there is a decrease of the signal compared to vehicle (VEH vs. SEL/BTZ/CO:  $p$ -value  $<0.0001$ ), as well as between single agents and dual therapy (SEL/BTZ vs. CO:  $p$ -value  $<0.05$ ). **b–c.** IMR5 and NLF cell lines were treated with vehicle, selinexor, bortezomib, and combination with each of 3 knockdown conditions: 1) non-targeting (NT) siRNA, 2) siRNA targeting Ikb construct 1 (siRNA1), and 3) siRNA targeting Ikb construct 2 (siRNA2). Representative Western blots of knockdown achieved are shown. With the NT siRNA and the single/combo treatments, cellular proliferation was expectedly decreased (IMR5 – SEL/BTZ: siRNA1  $p$ -value  $<0.01$ , siRNA2  $p$ -value  $<0.05$ ; NLF – SEL: siRNA1  $p$ -value  $<0.05$ , siRNA2  $p$ -value  $<0.01$ , BTZ: siRNA1  $p$ -value  $<0.001$ ), while siRNA 1 and 2 diminished this effect (IMR5 – CO: siRNA1  $p$ -value  $<0.01$ , siRNA 2  $p$ -value  $<0.05$ ; NLF – CO: siRNA1  $p$ -value  $<0.05$  and siRNA2  $p$ -value  $<0.05$ ). In response to Ikb knockdown, the selinexor effect on cellular proliferation was similar to vehicle, while bortezomib and combination treatment resulted in an increase in cellular activity.  $p$ -values correspond to  $<0.05$ -\*,  $<0.01$ -\*\*,  $<0.001$ -\*\*\*,  $<0.0001$ -\*\*\*\* and all experiments shown are 4 replicates with 3 technical replicates per condition for luciferase and 6 technical replicates for proliferation assays.

tion in the NF-kB inhibitory complex in the cytoplasmic compartment [39,48]. Bortezomib is now integrated into standard of care across a range of adult malignancies yet it has underperformed in neuroblastoma studies. With the knowledge that Ikb is a cargo protein of selinexor, we investigated the use of selinexor and bortezomib in combination, building on prior work in multiple myeloma [39,40,49]. Ikb in the nucleus would be expected to inhibit the transcription factor NF-kB and thereby change the dynamics of downstream targets that promote cancer survival in neuroblastoma. We demonstrated that Ikb is a key mediator of the synergistic effect of combination therapy on NF-kB activity in neuroblastoma. Although siRNA knockdown of Ikb ablated the effect of selinexor, knockdown of Ikb promoted the proliferation of cells treated with bortezomib, possibly because stabilization by bortezomib of other proteins that are degraded by the proteasome, results in stimulation of NF-kB activity in the absence of Ikb, as NF-kB transcription factor signaling networks can both promote or suppress growth [50,51]. Understanding these complexities will be crucial for the development of this treatment for patients with neuroblastoma, in particular because resistance to selinexor in multiple myeloma, for example, is associated with increased NF-KB activity [45].

An important finding from this work is that the synergy between selinexor and bortezomib is independent of *TP53* mutation status or *MYCN* amplification status. These two molecular aberrations are associated with aggressive disease and relative chemoresistance. *TP53* is typically wild type in newly diagnosed neuroblastoma, but in relapsed disease can mutate (e.g., NLF cell line is a representation of this phenomenon), and hamper therapeutic responses [52,53]. *TP53* is also a cargo protein of XPO1 and diminished nuclear abundance correlates with diminished tumor suppression in patients [54–56]. *MYCN* is similarly an elusive target in neuroblastoma, with the oncogene amplified in about half of patients with high-risk neuroblastoma. *MYCN* is known to activate numerous genes involved in the promotion and maintenance of cancer and stemness [57]. While cell lines responded to combination therapy regardless of *MYCN* status, the *MYCN* non-amplified cell line, SKNSH, demonstrated an inclination towards an increase in cell cycle arrest in response to selinexor and bortezomib. Interestingly, SKNSH has increased levels of Cyclin D1, a protein involved in cell cycle regulation, and the expression of this protein changes as the cell proceeds through G1/S phase transition [58,59]. Increased levels and activity of Cyclin D1 contribute to a less differentiated phenotype, and loss of Cy-

clin D1 expression leads to cell cycle arrest and apoptosis [60,61]. The different mechanisms affecting cellular processes in response to combination therapy, including determinants of cell cycle inhibition, in *MYCN* amplified versus non-amplified lines is a focus of ongoing investigation.

In summary, we have demonstrated that high XPO1 protein expression correlates with an inferior outcome in neuroblastoma. In patient-derived neuroblastoma cells that represent the heterogeneous nature of this cancer, there is synergistic inhibition of cellular proliferation with the use of selinexor and bortezomib. This is mediated, at least in part, by I $\kappa$ B regulation of the NF- $\kappa$ B signaling pathway. Our findings demonstrate that XPO1 is a potential prognostic biomarker and reveal a targeted therapeutic approach, that can be integrated into the next generation of clinical trials. Ongoing work is focused on patient-derived xenograft in vivo testing of selinexor/bortezomib combinatorial strategies, as well as studies to understand how XPO1 overexpression promotes aggressive neuroblastoma. We will also assess dose reduction of bortezomib and/or selinexor when used in combination, similar to approaches used in multiple myeloma to increase tolerability [62]. Results from this work, combined with exploration of gene expression changes in response to single agents and combination therapy, will provide additional insight about our therapeutic strategy that addresses current challenges in treating highly aggressive neuroblastoma.

#### Declaration of Competing Interest

The authors declare the following financial interests/personal relationships which may be considered as potential competing interests.

#### CRedit authorship contribution statement

**Basia Galinski:** Data curation, Writing - original draft, Visualization, Investigation, Formal analysis, Validation, Project administration. **Marcus Luxemburg:** Data curation, Investigation. **Yosef Landesman:** Resources, Supervision. **Bruce Pawel:** Investigation. **Katherine J. Johnson:** Data curation. **Stephen R. Master:** Investigation. **Kevin W. Freeman:** Writing - review & editing, Validation. **David M. Loeb:** Writing - review & editing, Validation, Supervision. **Jean M. Hébert:** Writing - review & editing, Supervision. **Daniel A. Weiser:** Conceptualization, Writing - review & editing, Visualization, Funding acquisition, Project administration, Supervision.

#### Acknowledgments

This study was supported by Hyundai Hope on Wheels (DW) and the Sneider family (DW). Funding was also provided by U24CA196173/114766 (COG Biopathology Center) and U10CA180899 (COG Statistics and Data Center), and we thank the Children's Oncology Group for providing patient samples. This work utilized the Leica SP8 confocal and BD Bioscience LSRII benchtop confocal which were purchased through funding from NIH SIG grant 1S10OD023591-01 and NCI support grant P30CA01330, respectively. We would like to thank Dr. Raquel Castellanos and Philip Galbo M.S. for their intellectual contributions to the laboratory.

#### Consent

Our study of tumor material from patients was granted exempt status by the institutional review board.

#### Supplementary materials

Supplementary material associated with this article can be found, in the online version, at [doi:10.1016/j.tranon.2021.101114](https://doi.org/10.1016/j.tranon.2021.101114).

#### Bibliography

- [1] J.M. Maris, K.K. Matthay, Molecular biology of neuroblastoma, *J. Clin. Oncol.* 17 (1999) 2264–2279.
- [2] M.A. Escobar, et al., Long-term outcomes in patients with stage IV neuroblastoma, *J. Pediatr. Surg.* 41 (2006) 377–381.
- [3] K.R. Bosse, J.M. Maris, Advances in the translational genomics of neuroblastoma: from improving risk stratification and revealing novel biology to identifying actionable genomic alterations, *Cancer* 122 (2016) 20–33.
- [4] B. Koneru, et al., Telomere maintenance mechanisms define clinical outcome in high-risk neuroblastoma, *Cancer Res.* (2020), doi:10.1158/0008-5472.CAN-19-3068.
- [5] F. Zhou, et al., CRM1 is a novel independent prognostic factor for the poor prognosis of gastric carcinomas, *Med. Oncol.* 30 (2013) 726.
- [6] A. Shen, et al., Expression of crm1 in human gliomas and its significance in P27 expression and clinical prognosis, *Neurosurgery* 65 (2009) 153–160.
- [7] A. Noske, et al., Expression of the nuclear export protein chromosomal region maintenance/exportin 1/Xpo1 is a prognostic factor in human ovarian cancer, *Cancer* 112 (2008) 1733–1743.
- [8] J. Schmidt, et al., Genome-wide studies in multiple myeloma identify XPO1/CRM1 as a critical target validated using the selective nuclear export inhibitor KPT-276, *Leukemia* 27 (2013) 2357–2365.
- [9] R. Sexton, et al., Targeting nuclear exporter protein XPO1/CRM1 in gastric cancer, *Int. J. Mol. Sci.* 20 (2019).
- [10] E.F. Attiyeh, et al., Pharmacodynamic and genomic markers associated with response to the XPO1/CRM1 inhibitor selinexor (KPT-330): a report from the pediatric preclinical testing program, *Pediatr. Blood Cancer* 63 (2016) 276–286.
- [11] G.L. Gravina, et al., Nucleo-cytoplasmic transport as a therapeutic target of cancer, *J. Hematol. Oncol.* 7 (2014) 85.
- [12] J. Ishizawa, K. Kojima, N. Hail, Y. Tabe, M. Andreeff, Expression, function, and targeting of the nuclear exporter chromosome region maintenance 1 (CRM1) protein, *Pharmacol. Ther.* 153 (2015) 25–35.
- [13] K. Stade, C.S. Ford, C. Guthrie, K. Weis, Exportin 1 (Crm1p) is an essential nuclear export factor, *Cell* 90 (1997) 1041–1050.
- [14] N. Kudo, et al., Leptomycin B inhibition of signal-mediated nuclear export by direct binding to CRM1, *Exp. Cell Res.* 242 (1998) 540–547.
- [15] A. Chari, et al., Oral selinexor-dexamethasone for triple-class refractory multiple myeloma, *N. Engl. J. Med.* 381 (2019) 727–738.
- [16] R. Nakayama, et al., Preclinical activity of selinexor, an inhibitor of XPO1, in sarcoma, *Oncotarget* 7 (2016) 16581–16592.
- [17] J. Kuruvilla, et al., The oral selective inhibitor of nuclear export (SINE) selinexor (KPT-330) demonstrates broad and durable clinical activity in relapsed/refractory Non Hodgkin's Lymphoma (NHL), *Blood* (2014).
- [18] S. Ben-Barouch, J. Kuruvilla, Selinexor (KTP-330) – a selective inhibitor of nuclear export (SINE): anti-tumor activity in diffuse large B-cell lymphoma (DLBCL), *Exp. Opin. Investig. Drugs* 29 (2020) 15–21.
- [19] Y.Y. Syed, Selinexor: first global approval, *Drugs* 79 (2019) 1485–1494.
- [20] R.E. Brown, et al., Morphoproteomic confirmation of constitutively activated mTOR, ERK, and NF-kappaB pathways in high risk neuro-blastoma, with cell cycle and protein analyte correlates, *Ann. Clin. Lab. Sci.* 37 (2007) 141–147.
- [21] X. Bian, et al., Constitutively active NFkappa B is required for the survival of S-type neuroblastoma, *J. Biol. Chem.* 277 (2002) 42144–42150.
- [22] S. Chen, et al., Genome-wide siRNA screen for modulators of cell death induced by proteasome inhibitor bortezomib, *Cancer Res.* 70 (2010) 4318–4326.
- [23] M. Michaelis, et al., Anti-cancer effects of bortezomib against chemoresistant neuroblastoma cell lines in vitro and in vivo, *Int. J. Oncol.* 28 (2006) 439–446.
- [24] C. Brignole, et al., Effect of bortezomib on human neuroblastoma cell growth, apoptosis, and angiogenesis, *J. Natl. Cancer Inst.* 98 (2006) 1142–1157.
- [25] U. Valentiner, C. Haane, N. Nehmann, U. Schumacher, Effects of bortezomib on human neuroblastoma cells in vitro and in a metastatic xenograft model, *Anticancer Res.* 29 (2009) 1219–1225.
- [26] B. Piperdi, Y.-H. Ling, L. Liebes, F. Muggia, R. Perez-Soler, Bortezomib: understanding the mechanism of action, *Mol. Cancer Ther.* 10 (2011) 2029–2030.
- [27] K.J. Heaton, S.R. Master, Peptide extraction from formalin-fixed paraffin-embedded tissue, *Curr. Protoc. Protein Sci.* (2011) **Chapter 23**, Unit23.5.
- [28] J.R. Wiśniewski, A. Zougman, N. Nagaraj, M. Mann, Universal sample preparation method for proteome analysis, *Nat. Methods* 6 (2009) 359–362.
- [29] J. Rappsilber, M. Mann, Y. Ishihama, Protocol for micro-purification, enrichment, pre-fractionation and storage of peptides for proteomics using StageTips, *Nat. Protoc.* 2 (2007) 1896–1906.
- [30] Y.V. Karpievitch, A.R. Dabney, R.D. Smith, Normalization and missing value imputation for label-free LC-MS analysis, *BMC Bioinform.* 13 (Suppl 16) (2012) S5.
- [31] A.D. Polpitiya, et al., DANTE: a statistical tool for quantitative analysis of -omics data, *Bioinformatics* 24 (2008) 1556–1558.
- [32] R. Suzuki, H. Shimodaira, Pvcust: an R package for assessing the uncertainty in hierarchical clustering, *Bioinformatics* 22 (2006) 1540–1542.
- [33] Y. Chen, et al., Inhibition of the nuclear export receptor XPO1 as a therapeutic target for platinum-resistant ovarian cancer, *Clin. Cancer Res.* 23 (2017) 1552–1563.
- [34] M. Deng, et al., XPO1 expression worsens the prognosis of unfavorable DLBCL that can be effectively targeted by selinexor in the absence of mutant p53, *J. Hematol. Oncol.* 13 (2020) 148.
- [35] U.H. Gandhi, et al., Clinical implications of targeting XPO1-mediated nuclear export in multiple myeloma, *Clin. Lymphoma Myeloma Leuk.* 18 (2018) 335–345.
- [36] K. Kojima, et al., Prognostic impact and targeting of CRM1 in acute myeloid leukemia, *Blood* 121 (2013) 4166–4174.

- [37] M.J. Tariq, et al., Clinical response and tolerability of selinexor in acute myeloid leukemia and other hematologic malignancies – a systematic review, *Blood* 132 (2018) 5231–5231.
- [38] R. Mody, L. Zhao, G.A. Yanik, V. Pipari, Phase I study of bortezomib in combination with irinotecan in patients with relapsed/refractory high-risk neuroblastoma, *Pediatr. Blood Cancer* 64 (2017).
- [39] J.G. Turner, et al., XPO1 inhibitor combination therapy with bortezomib or carfilzomib induces nuclear localization of  $I\kappa B\alpha$  and overcomes acquired proteasome inhibitor resistance in human multiple myeloma, *Oncotarget* 7 (2016) 78896–78909.
- [40] N.J. Bahlis, et al., Selinexor plus low-dose bortezomib and dexamethasone for patients with relapsed or refractory multiple myeloma, *Blood* 132 (2018) 2546–2554.
- [41] J. Yang, et al., The essential role of MEKK3 in TNF-induced NF- $\kappa$ B activation, *Nat. Immunol.* 2 (2001) 620–624.
- [42] A.R. Abdul Razak, et al., First-in-class, first-in-human phase I study of selinexor, a selective inhibitor of nuclear export, in patients with advanced solid tumors, *J. Clin. Oncol.* 34 (2016) 4142–4150.
- [43] W. Gao, C. Lu, L. Chen, P. Keohavong, Overexpression of CRM1: a characteristic feature in a transformed phenotype of lung carcinogenesis and a molecular target for lung cancer adjuvant therapy, *J. Thorac. Oncol.* 10 (2015) 815–825.
- [44] M. Aladhraei, A. Kassem Al-Thobhani, N. Pongvarin, P. Suwannalert, Association of XPO1 overexpression with NF- $\kappa$ B and Ki67 in colorectal cancer, *Asian Pac. J. Cancer Prev.* 20 (2019) 3747–3754.
- [45] T. Kashyap, et al., Efficacy of selinexor is dependent on  $I\kappa B\alpha$  expression and NF- $\kappa$ B deactivation in multiple myeloma cells, *Blood* 128 (22) (2016) 5660.
- [46] J.S. Nair, E. Musi, G.K. Schwartz, Selinexor (KPT-330) induces tumor suppression through nuclear sequestration of  $I\kappa B$  and downregulation of survivin, *Clin. Cancer Res.* 23 (2017) 4301–4311.
- [47] X. Dolcet, D. Llobet, J. Pallares, X. Matias-Guiu, NF- $\kappa$ B in development and progression of human cancer, *Virchows Arch.* 446 (2005) 475–482.
- [48] J.A. DeSisto, et al., Exportin 1 inhibition induces nerve growth factor receptor expression to inhibit the NF- $\kappa$ B pathway in preclinical models of pediatric high-grade glioma, *Mol. Cancer Ther.* 19 (2020) 540–551.
- [49] D.M. Sullivan, et al., Combination therapy of selinexor with bortezomib or carfilzomib overcomes drug resistance to proteasome inhibitors (PI) in human multiple myeloma, *Blood* 126 (23) (2015) 3048.
- [50] P. Godwin, et al., Targeting nuclear factor- $\kappa$ B to overcome resistance to chemotherapy, *Front. Oncol.* 3 (2013) 120.
- [51] Y. Zhi, et al., NF- $\kappa$ B signaling pathway confers neuroblastoma cells migration and invasion ability via the regulation of CXCR4, *Med. Sci. Monit.* 20 (2014) 2746–2752.
- [52] V.V. Subhash, et al., Anti-tumor efficacy of selinexor (KPT-330) in gastric cancer is dependent on nuclear accumulation of p53 tumor suppressor, *Sci. Rep.* 8 (2018) 12248.
- [53] X. Ling, D. Calinski, A.A. Chanan-Khan, M. Zhou, F. Li, Cancer cell sensitivity to bortezomib is associated with survivin expression and p53 status but not cancer cell types, *J. Exp. Clin. Cancer Res.* 29 (8) (2010).
- [54] N. Keshelava, et al., Loss of p53 function confers high-level multidrug resistance in neuroblastoma cell lines, *Cancer Res.* 61 (2001) 6185–6193.
- [55] D.A. Tweddle, A.J. Malcolm, N. Bown, A.D. Pearson, J. Lunec, Evidence for the development of p53 mutations after cytotoxic therapy in a neuroblastoma cell line, *Cancer Res.* 61 (2001) 8–13.
- [56] U.M. Moll, et al., Cytoplasmic sequestration of wild-type p53 protein impairs the G1 checkpoint after DNA damage, *Mol. Cell. Biol.* 16 (1996) 1126–1137.
- [57] M. Huang, W.A. Weiss, Neuroblastoma and MYCN, *Cold SpringHarb. Perspect. Med.* 3 (2013) a014415.
- [58] J.J. Molenaar, P. van Sluis, K. Boon, R. Versteeg, H.N. Caron, Rearrangements and increased expression of cyclin D1 (CCND1) in neuroblastoma, *Genes Chromosom. Cancer* 36 (2003) 242–249.
- [59] R. Donnellan, R. Chetty, Cyclin D1 and human neoplasia, *Mol. Pathol.* 51 (1998) 1–7.
- [60] L.J. Wainwright, A. Lasorella, A. Iavarone, Distinct mechanisms of cell cycle arrest control the decision between differentiation and senescence in human neuroblastoma cells, *Proc. Natl. Acad. Sci. USA* 98 (2001) 9396–9400.
- [61] J.J. Molenaar, et al., Cyclin D1 and CDK4 activity contribute to the undifferentiated phenotype in neuroblastoma, *Cancer Res.* 68 (2008) 2599–2609.
- [62] B. Muz, F. Azab, P. de la Puente, Y. Landesman, A.K. Azab, Selinexor overcomes hypoxia-induced drug resistance in multiple myeloma, *Transl. Oncol.* 10 (2017) 632–640.